Nonlin. Processes Geophys. Discuss., https://doi.org/10.5194/npg-2019-8
Manuscript under review for journal Nonlin. Processes Geophys.
Discussion started: 27 March 2019

Nonlinear Processes in Geophysics
Discussions
Open Access

Application of fractal models to delineate mineralized zones in the Pulang porphyry copper deposit,Yunnan, Southwest China

Xiaochen Wang[a], Qinglin Xia[a,b,*], Tongfei Li[a], Shuai Leng[a], Yanling Li[a], Li Kang[a], Zhijun Chen[a], Lianrong Wu[c]

[a] Faculty of Earth Resources, China University of Geosciences, Wuhan 430074, China

[b]Collaborative Innovation Center for Exploration of Strategic Mineral Resources, Wuhan 430074, China

[c]Yunnan Diqing Nonferrous MetalCo., Ltd., Shangri-La674400, China

Abstract

The purpose of the paper is to depict various mineralized zones and the barren host rock in accordance with the subsurface and surface lithogeochemical data using the concentration–volume (C–V) and power spectrum–volume (S–V) fractal models within the Pulang copper deposit, southwest China. Results obtained by concentration–volume model depict four geochemical zones defined by Cu thresholds of 0.25%, 1.38% and 1.88%, which represent non-mineralized wall rocks (Cu<0.25%), weakly mineralized zones (0.25%–1.38%), moderately mineralized zones (1.38%–1.88%), and highly mineralized zones (Cu>1.88%).S–V model is utilized by performing 3D fast Fourier transformation for assay data in the frequency domain. The S–V method indicates three mineralized zones characterized by Cu threshold valuesof 0.23% and 1.33%. The zones of <0.23% Cu represent barren host rocks and zonesof 0.23%-1.33% Cu represent the hypogene zones and zones >1.33% Cu represent supergene enrichment zones. Both the multifractal models show that high grade mineralization is located at the center and south of Pulang deposit. The results are in contrast with alteration and mineralogical models resulted from the 3D geologic model utilizing the logratio matrix method. Better results were obtained from S–V model to delineate high grade mineralization of Pulang deposit.However, results of C–V method of moderate and weak grade mineralization are more precise than the results gained from S–V method.

Keywords:Fractal; Concentration–volume model (C–V); Power spectrum–volume model (S–V); Mineralized zone; the Pulang porphyry copper deposit

1. Introduction

The depiction and recognization of various mineralized zones and barren host rock is the primary goal of the mineral exploration work. The research of systematic ore-forming mineralogy offers helpful data about the metallogenic processes of deposits, for the mineral assemblages of different types of deposits reflect the typical characteristics (White and Hedenquist, 1995; Craig andVaughan, 1994).Common means are on the basis of mineralography, petrography and alteration minerals assemblages to delineate various mineralized zones in porphyry deposits (Beane, 1982; Schwartz, 1947;Sillitoe, 1997; Berger et al., 2008). Lowell(1968) firstly put forward a theory model which indicated the mineralogy variations of lateral and vertical directions in the alteration zones. Some comparable models are usually proposed related to potassic zones frequently situated in the center and deep of porphyry ore deposits on the basis of this model (Sillitoe and Gappe, 1984; Cox and Singer, 1986;Melfos et al., 2002).There are also other methods such as stable isotope studies and fluid inclusion to outline various mineralization phases(Boyce et al., 2007; Wilson et al., 2007). The drillhole data with logging information containing mineralographical information, host rock changes and alteration is helpful to delineate the mineralization zones. The boundaries of different zones can be exhibited by different geological interpretations and various results can be obtained.

Non-Euclidian fractal geometry is an significant branch of non-linear sciences. It is utilized in various research fields of geosciences since 1980s (Mandelbrot, 1983).The correlations between geology, geochemistry and mineralogical backgrounds with spatial information can be researched by the methods on the basis of fractal geometry (Carranza,2008, 2009). The fact that the fractal dimensions exist in different geochemical patterns of diverse elements has been shown by Bolviken et al. (1992) and Cheng et al. (1994). The concentration–area(C–A) fractal method was put forward by Cheng et al. (1994) to recognize geochemical anomalies from backgrounds and calculate thresholds of geochemical data of different elements. Furthermore, there are many other fractal methods proposed and utilized in exploration work of geochemistry including number–size (N–S) fractal method proposed by Mandelbrot (1983), concentration–perimeter(C–P) fractal method proposed by Cheng (1995), power spectrum–area(S–A) fractal method proposed by Cheng et al.(1999), concentration–distance (C–D)fractal method proposed by Li et al.(2003), concentration–volume (C–V) fractal method proposed by Afzal et al.(2011) and power spectrum–volume (S–V) fractal method proposed by Afzal et al.(2012). Different geochemical processes could be described by the diversities within fractal dimensions, which obtained by research of relative geochemical data. Afzal et al.(2011) considered that the log–log plots obtained by fractal methods are useful means to delineate different populations of geochemical data and the thresholds could be determined as some break points in plots.

The utilization of fractal models to delineate various grade mineralization is dependent on the correlations of metal grades and volumes (Afzal et al., 2011; Cheng, 2007; Simet al., 1999; Agterberg et al., 1993). The concentration–volume (C–V) and power spectrum–volume (S–V) fractal methods were put forward by Afzal et al. (2011, 2012) to delineate various grade mineralization. We utilized C–V and S–V fractal methods to delineate diverse mineralized zones and host rocks of Pulang copper deposit within this paper.

2. Fractal models

2.1. Concentration–volume fractal model

Afzal et al. put forward concentration–volume fractal method in 2011 based on the same principle of the concentration–area method (Cheng et al., 1994) in order to analysis the correlation between the concentration of ore elements and relevant occupied volume which its concentration is above or less than the presented value (Afzal et al., 2011;Sadeghi et al., 2012; Soltani et al.,2014; Zuo et al., 2016).It could be shown as:

$$V(\rho\leq\upsilon)\propto\rho^{-a_1};\ V(\rho\geq\upsilon)\propto\rho^{-a_2} \quad (1)$$

V(ρ≥υ) and V(ρ≤υ) represent those occupied volumes which concentrations are above or equal to and less than or equal to presented value υ; υ indicates the threshold between two zones; a_1 and a_2 indicate the characteristic indexes.Thresholds obtained by this method indicate the boundaries of diverse grade mineralization of ore deposits. The drill hole data of elemental concentration values are interpolated with the method of geostatistical estimation to compute V(ρ≥υ) and V(ρ≤υ).They are those volume values surrounded with the given value υ within a 3D model.

2.2. Power spectrum–volumefractal model

Different geochemical patterns existed within spatial domain could be seen as layered signals with various frequencies.Cheng et al. (1999) put forward power spectrum–area fractal method to recognize geochemical anomalies from backgrounds utilizing the method of spectrum analysis within frequency domain according to this argument. This model is combined with concentration–area method (Cheng et al. 1994). It offers an useful mean to determine an optimum threshold value between various forms based on different scaling property.

Afzal et al.(2012) put forward power spectrum–volume (S–V) fractal method to delineate different grade mineralization based on the same idea as the S–A method proposed by Cheng et al.(1999).S–V method was utilized in frequency domain. And it was performed by applying the fast Fourier transformation for assay data. The straight lines obtained by log–log plots indicate the relationships between power spectrums and relative volumes of ore elements. They were utilized to recognize the hypogene zones and supergene zones from barren host rocks and leached zone of the deposit. The recognization of various mineralization zones is on the basis of the power–law correlations of power spectrums and relative volumes. The formula is as follows:

$$V(\geq S) \propto S^{-2/\beta} \tag{2}$$

Where, the relationships of power spectrums (S=−||F(Wx, Wy, Wz)||) and occupied volumes which power spectrums are greater than or equal to S can be indicated by this form; F represents the fast Fourier transformation for the measurement μ(x, y, z); Wx, Wy and Wz seperately indicate wavenumbers or angular frequencies of the directions of X, Y and Z axis of a 3D model.The range of index β is 0<β≤2 or 1≤2/β with particular circumstance of β=2 or 2/β=1 related to monofractal or non-fractal and 1<2/β to multifractal (Cheng, 2006).

By utilizing the method of geostatistical estimation, drill hole data of elemental concentration values are interpolated to construct the block model with ore element distribution. The power spectrum values can be obtained by utilizing 3D fast Fourier transformation for ore element grades.

The obtained data was classified to a number of classes. The determination of the amount of classes should consider the gross amount of data at a required precise level. The range value from the minimum to maximum values of power spectrum was calculated and the width of each class was finally decided by separating the range into the amount of classes. Then we count the amount of voxels of each class and compute their accumulative volume values. And all of the considered voxels are counted as points because they have constant volumes. The logarithm of all power spectrum values and accumulative volume values were calculated. And the log-log plot of power spectrums and volumes was drawed according to previous counted values. Then the filters were constructed on the basis of threshold values obtained by the log-log plot of S-V. Finally, the resulted power spectrums were converted back to space domain by utilizing inverse fast Fourier transformation.

3. The geological setting of Pulang copper deposit

The Pulang depositis situated in the southern end of Yidun continental arc of southwest China (Fig. 1). The continental arc is generated due to the westward subduction of Garze–Litang oceanic crust(Deng et al., 2014b, 2015; Wang et al., 2014). And Leng et al. (2012) and Li et al.(2011, 2013) have systematically researched detailed geological characteristics of Pulang deposit, such as the representative porphyry alteration zones, the geometry of orebody, metallogenic time and the geodynamic settings of this deposit.The Pulang deposit consists of five ore–bearing porphyries. They cover an range of about 9 square kilometers. Liu et al. (2013) showed that Cu ore tonnage of Pulang deposit is reckoned to be 6.50 Mt.

Nonlin. Processes Geophys. Discuss., https://doi.org/10.5194/npg-2019-8
Manuscript under review for journal Nonlin. Processes Geophys.
Discussion started: 27 March 2019

Nonlinear Processes in Geophysics
Open Access
Discussions

The outcrop strata of Pulang deposit mainly consist of clastic rocks, andesite and quaternary sediments of UpperTriassic Tumugou Formation (Fig.1c).The Triassic porphyry intrusions mainly comprise quartz monzonite porphyry, quartz diorite porphyry,quartz diorite porphyrite and granodiorite porphyry. The Tumugou Formation strata was intruded by the quartz diorite porphyry with an age of 219.6 ± 3.5 Ma obtained by Zircon U–Pb dating(Pang et al., 2009). Then quartz monzonite porphyry with an age of 212.8 ± 1.9 Ma and granodiorite porphyry with an age of 206.3 ± 0.7 Ma obtained by Zircon U–Pb dating (Liu et al., 2013) seperately crosscut quartz diorite porphyry.The quartz monzonite porphyry is related to mineralization for its age is similar with the Re–Os isochron age of 213 ± 3.8 Ma from molybdenite of deposit (Zeng et al., 2004). Moreover, the Cu grades of quartz monzonite porphyry are higher than the other porphyries.

<Fig. 1 inserts here>

The porphyry-type alteration zones transform from potassium–silication, quartz–sericitization to propylitization zones upward and outward from the center of quartz monzonite porphyry(Fig.4).Most country rocks close to the porphyries were transformed to hornfels. The fact that potassic and quartz–sericitization zones control most orebodies has been validated by the systematic drilling. They constitute the core of mineralized zones. And the weak mineralization often appear in the propylitic zones and hornfels surrounding the core.The orebodies occur as veins within the propylitic zones and hornfels.Major rock types in the deposit are quartz monzonite porphyry, quartz diorite porphyrite, granite diorite porphyry, quartz diorite porphyry and hornfels(Fig. 2). Metallic minerals mainly include chalcopyrite, pyrite and some molybdenite and pyrrhotite (Fig. 3).

<Fig. 2 inserts here>

<Fig. 3 inserts here>

<Fig. 4 inserts here>

4. Fractal modeling

Nonlin. Processes Geophys. Discuss., https://doi.org/10.5194/npg-2019-8
Manuscript under review for journal Nonlin. Processes Geophys.
Discussion started: 27 March 2019

On the basis of the geological data of this deposit, such as the collar coordinates, azimuth, dip, mineralogy and lithology of 130 drill holes, 19996 samples were gathered from these drill holes every other 2 meters. The laboratory of the 3rd geological team of Geology and Mineral Resources Bureau of YunnanDiqing Nonferrous Metal Co. Ltd. utilized iodine–fluorine and oscillo-polarographic method to analyze the concentrations of Cu and associated paragenetic elements of all the drill holes and its analytical uncertainty is less than 7%. Only Cu concentrations were researched in this study. The distribution of Cu concentrations is presented in Fig. 5 with Cu mean value of 0.296%. The experimental semi–variogram of Cu data of Pulang deposit indicates that these values of the nugget effect and range are 0.126 and 160.0m, seperately(Fig. 6).The spherical model is fitted in regard to the experimental semi–variogram.The 3D model of Cu concentrations dispersion of Pulang deposit is produced by utilizing ordinary kriging method of the Geovia Surpac on the basis of the semi–variogram and anisotropic ellipsoid. Goovaerts (1997) showed that the values in un-sampled locations are estimated by the ordinary kriging method according to moving average of interest variables fitting various distribution patterns of data.It is a spatial estimation means and its error variance related to characteristics and patterns of the data is minimized. The obtained block model by this method are utilized as input to fractal models.The Pulang deposit is modeled by 20m × 20m × 5m voxels and they are decided by the grid drilling dimensions and geometrical characteristics of the Pulang deposit (David, 1970). Pulang deposit is totally modeled with 150,973 voxels. Different mineralized zones are classified on the basis of these two fractal methods in this deposit.

<Fig. 5 inserts here>

<Fig. 6 inserts here>

4.1. Concentration–volume (C–V) fractal modeling

The occupied volume values related to Cu grades are computed to obtain the concentration–volume model according to the 3D model of Pulang deposit.Through the obtained log–log plot of concentrations vs volumes, the threshold values of Cu grades were determined (Fig.7). It indicates the power-law relation of Cu grades and volumes. Three thresholds and four populations are gained from C–V log–log plot, consequently. The first Cu threshold is 0.25%. The range of Cu values of <0.25% represent barren host rock.The second Cu threshold is 1.38%, and values of 0.25–1.38% Cu represent weak grade mineralization.And the third Cu threshold is 1.88%. The range of Cu values of 1.38–1.88% denote moderately mineralized zones, and values of >1.88% Cu indicate highly mineralized zones (Table 1). According to the results, the low concentration zones develop in a lot of sections of Pulang deposit and are inclined to the northwest–southeast direction of the deposit. Moderately and highly mineralized zones are located at several parts of the center and south of Pulang deposit(Fig. 8).

<Fig. 7 inserts here>

<Fig. 8 inserts here>

< Table 1 inserts here>

4.2. Power spectrum–volume (S–V) fractal modeling

According to the geological data from this deposit, such as the collar coordinates, azimuth, dip, mineralogy and lithology of 130 drill holes, a 3D model and block model of Cu grades dispersion of Pulang deposit were constructed by ordinary kriging method utilizing the Geovia Surpac.

The power spectrum (S) of Cu grades distribution are computed by utilizing 3D fast Fourier transformation by MATLAB (R2016a). The logarithmic values of power spectrum and relevant volume values are fitted against each other (Fig. 9). The straight lines fitted through the log–log plot indicate the relation of power spectrums and occupied volumes. The results have indicated that there are two thresholds and three populations. The thresholds of logS=7.81 and logS=8.70 are decided by the log–log S–V plot. The 3D filters were designed to separate different mineralization zones on the basis of these threshold values. Inverse fast Fourier transformation was utilized to convert the resulted power spectrums back into space domain by MATLAB (R2016a). According to the results, Cu grades of hypogene zones range from 0.23% to 1.33% (Table 2), and values of >1.33% Cu refer to the supergene enrichment zones, whereas values of <0.23% Cu pertain to the leached zone and barren host rock(Fig. 10).

<Fig. 9 inserts here>

<Fig. 10 inserts here>

< Table 2 inserts here>

5. The contrast of results of fractal models and geologic models of Pulangdeposit

Lowell and Guilbert(1970) depicted that the alteration models are very critical within zone recognization. The potassic and phyllic alterations control the most mineralization within supergene and hypogene zones according to these models. The various mineralization zones obtained by the fractal methods could be in contrast with geologic data to verify these results.

Results of fractal models of Pulang deposit were in contrast with 3D geologic model of Pulang deposit constructed by utilizing Geovia Surpac and drillholes data (Fig. 2). Furthermore, results gained from fractal models are also dominated by mineralogical research.

The analysis of spatial relationships of two binary particularly geology and mathematics models has been indicated by Carranza (2011).The intersection operation between the mineralization zones obtained from fractal models and alteration zones is carried out to derive the amount of voxels related to every class of overlap zones (Table3). And overall accuracy (OA) values of different grade mineralization obtained by these fractal methods are in contrast with each other.

The contrast between highly mineralized zones on the basis of the fractal models and potassic zones resulted from 3D geologic model illustrates that the results of these two fractal models are similar.The OA values of C–V and S–V methods are 0.50 and 0.52 as shown in Table 4, which illustrate that the S–V model gets more accurate results to recognize high grade mineralization of Pulang deposit.

The contrast between phyllic alteration zones resulted from 3D geologic model and moderate grade mineralization obtained from fractal methods indicates that OA values of C–V and S–V fractal methods in regard to phyllic alteration zones of the geological model are 0.59 and 0.56 (Table 5). The OA values of moderate and weak grade mineralization zones gained from C–V model is better than the results gained by S–V model.

It could be considered that there are spatial correlations between different grade mineralization and geologic features for instance alterations and mineralogy. Several samples of drillholes are gathered from different grade mineralization zones of Pulang deposit to validate the results of fractal models. PL-B82 was collected from supergene enrichment zones with high chalcopyrite content (Fig.13a). PL-B62 and PL-B74 samples were collected from the hypogene zones with low chalcopyrite content and some pyrrhotite content, respectively (Fig.13b and Fig.13c). PL-B94 sample was collected from leached zone and barren host rock with lower and no chalcopyrite content (Fig.13d).

<Fig. 11 inserts here>

<Fig. 12 inserts here>

<Fig. 13 inserts here>

6. Conclusions

This study utilized the concentration–volume(C–V) and power spectrum–volume (S–V) fractal models to delineate and recognize different grade Cu mineralization of Pulang copper deposit. Both the fractal models reveal high grade Cu mineralization is located at the center and south of Pulang deposit.The Cu threshold of high grade mineralization is 1.88% according to C–V method. And Cu threshold of supergene enrichment zones is 1.33% on the basis of S–V method. Models of moderate grade mineralization zones contain 1.38–1.88% Cu due to C–V method. And the hypogene zones contain 0.23–1.33% Cu according to the S–V model.

The C–V method shows barren host rock includes <0.25% and weak grade mineralization include 0.25–1.38% Cu. And the S–V model reveals that barren host rock and leached zone contain <0.23% Cu.

The high grade Cu mineralization determined by fractal methods, specially by

S–V method, give better relations with potassic zones of the 3D geologic model based on the relationship between results obtained from fractal methods and geologic logging of drill holes of Pulang deposit. In addition, there is a better correlation of moderate and weak grade mineralization obtained from C–V method and phyllic alteration zones based on the 3D geologic model.

< Table 3 inserts here>

< Table 4 inserts here>

< Table 5 inserts here>

Acknowledgements

This research was supported by the National Key R&D Program of China (2016YFC0600508). The authors thank Tao Dong, Haijun Yu, Qiwu Shen, Zhipeng Li, Baosheng Shi and Jinhong Yang for supporting in field investigation and providing parts of raw data.

Nonlin. Processes Geophys. Discuss., https://doi.org/10.5194/npg-2019-8
Manuscript under review for journal Nonlin. Processes Geophys.
Discussion started: 27 March 2019

Nonlinear Processes in Geophysics
Discussions

References

Agterberg, F.P., Cheng, Q., and Wright, D.F.: Fractal modeling of mineral deposits,in:Proceedings of the 24th APCOM Symposium, Montreal, Canada,43–53, 1993.

Agterberg, F.P.: Multifractal modeling of the sizes and grades of giant and supergiant deposits, International Geology Review, 37,1–8, https://doi.org/10.1080/00206819509465388 , 1995.

Agterberg, F.P., Cheng, Q., Brown, A., and Good, D.: Multifractal modeling of fractures inthe Lac du Bonnet Batholith, Manitoba, Comput. Geosci., 22, 497–507, https://doi.org/10.1016/0098-3004(95)00117-4, 1996.

Afzal, P., Khakzad, A., Moarefvand, P., Rashidnejad Omran, N., Esfandiari, B., and FadakarAlghalandis, Y.: Geochemical anomaly separation by multifractal modelingin Kahang (Gor Gor) porphyry system, Central Iran, J. Geochem. Explor., 104, 34–46, https://doi.org/10.1016/j.gexplo.2009.11.003, 2010.

Afzal, P., Fadakar Alghalandis, Y., Khakzad, A., Moarefvand, P., and Rashidnejad Omran, N.: Delineation of mineralization zones in porphyry Cu deposits by fractal concentration–volume modeling, J. Geochem. Explor., 108, 220–232, https://doi.org/10.1016/j.gexplo.2011.03.005, 2011.

Afzal, P., Fadakar Alghalandis, A., Moarefvand, P., Rashidnejad Omran, N., and Asadi Haroni, H.: Application of power–spectrum–volume fractal method for detecting hypogene, supergene enrichment, leached and barren zones in Kahang Cu porphyry deposit, Central Iran, J. Geochem. Explor., 112, 131–138, https://doi.org/10.1016/j.gexplo.2011.08.002, 2012.

Beane, R.E.: Hydrothermal alteration in silicate rocks, in: Advances in Geology of the Porphyry Copper Deposits, Southwestern NorthAmerica, Titley, S.R. (Ed.),The University of Arizona Press, Tucson, 117–137, 1982.

Bolviken, B., Stokke, P.R., Feder, J., and Jossang, T.: The fractal nature of geochemical landscapes, J. Geochem. Explor., 43,91–109,https://doi.org/10.1016/0375-6742(92)90001-O, 1992.

Nonlin. Processes Geophys. Discuss., https://doi.org/10.5194/npg-2019-8
Manuscript under review for journal Nonlin. Processes Geophys.
Discussion started: 27 March 2019

Nonlinear Processes in Geophysics
Open Access
Discussions

Boyce, A.J., Fulgnati, P., Sbrana, A., and Fallick, A.E.: Fluids in early stage hydrothermal alteration of high-sulfidation epithermal systems: a view from the volcano active hydrothermal system (Aeolian Island, Italy), Journal of Volcanology and Geothermal Research, 166, 76–90,https://doi.org/10.1016/j.jvolgeores. 2007.07.005, 2007.

Berger, B. R., Ayuso, R. A., Wynn, J. C., and Seal, R. R.: Preliminary Model of Porphyry Copper Deposits, USGS, Open-File Report, 1321 pp., 2008.

Bai, J., Porwal, A., Hart, C., Ford, A., and Yu, L.: Mapping geochemical singularity using multifractal analysis: application to anomaly definition on stream sediments data from Funin Sheet, Yunnan, China, J. Geochem. Explor., 104, 1–11,https://doi.org/10.1016/j.gexplo.2009.09.002, 2010.

Benndorf, J. and Dimitrakopoulos, R.: Stochastic long-term production scheduling ofiron ore deposits: Integrating joint multi-element geological uncertainty, J. Min. Sci., 49 (1), 68–81, https://doi.org/10.1134/S1062739149010097, 2013.

Cox, D. and Singer, D.: Mineral deposits models, US GeologicalSurvey Bulletin, 1693 pp., 1986.

Craig, G.R. and Vaughan, D.: Ore Microscopy and Ore Petrography, John Wiley andSons, 1994.

Chilès, J.P. and Delfiner, P.: Geostatistics: Modeling Spatial Uncertainty, Wiley, NewYork, 695 pp., 1999.

Carranza, E.J.M.: Geochemical Anomaly and Mineral Prospectivity Mapping inGIS. Handbook of Exploration and Environmental Geochemistry,11, Amsterdam, Elsevier, 351 pp., 2008.

Carranza, E. J. M.: Controls on mineral deposit occurrence inferredfrom analysis of their spatial pattern and spatial association withgeological features, Ore Geol. Rev., 35, 383–400, https://doi.org/10.1016/j.oregeorev.2009.01.001, 2009.

Carranza, E.J.M., Owusu, E.A., and Hale, M.: Mapping of prospectivity and estimationof number of undiscovered prospects for lode gold, southwestern Ashanti Belt, Ghana, Mineralium Deposita, 44, 915–938, https://doi.org/10.1007/ s00126-009-0250-6, 2009.

Nonlin. Processes Geophys. Discuss., https://doi.org/10.5194/npg-2019-8
Manuscript under review for journal Nonlin. Processes Geophys.
Discussion started: 27 March 2019

Nonlinear Processes in Geophysics
Discussions
Open Access
EGU

Carranza, E.J.M.: From predictive mapping of mineral prospectivity to quantitative estimation of number of undiscovered prospects, Resource Geology, 61, 30–51, https://doi.org/10.1111/j.1751-3928.2010.00146.x, 2010.

Carranza, E.J.M.: Analysis and mapping of geochemical anomalies using logratio-transformed stream sediment data with censored values, J. Geochem. Explor., 110, 167–185, https://doi.org/10.1016/j.gexplo.2011.05.007, 2011.

Cheng, Q., Agterberg, F.P., and Ballantyne, S.B.: The separation of geochemical anomaliesfrom backgroundby fractal methods, J. Geochem. Explor., 51, 109–130, https://doi.org/10.1016/0375-6742(94)90013-2, 1994.

Cheng, Q.: Spatial and scaling modelling for geochemical anomaly separation, J. Geochem. Explor., 65, 175–194, https://doi.org/10.1016/S0375-6742(99)00028-X, 1999.

Cheng, Q.: Mapping singularities with stream sediment geochemical data forprediction of undiscovered mineral deposits in Gejiu, Yunnan Province, China, Ore Geol. Rev., 32, 314–324,https://doi.org/10.1016/j.oregeorev.2006.10.002, 2007.

Chouinard, A., Williams-Jones, A.E., Leonardson, R.W., and Hodgson, C.J.: Geology andgenesis of the multistage high-sulfidation epithermal Pascua Au–Ag–Cu deposit, Chile and Argentina, Economic Geology, 100, 463–490,https://doi.org/10.2113/gsecongeo.100.3.463, 2005.

David, M.: Geostatistical Ore Reserve Estimation, Amsterdam, Elsevier, 283 pp., 1970.

Deng, J., Wang, Q.F., Yang, L.Q., Wang, Y.R., Gong, Q.J., and Liu, H.: Delineation andexplanation of geochemical anomalies using fractal models in the Heqing area,Yunnan province, China, J. Geochem. Explor., 105, 95–105,https://doi.org/10.1016/j.gexplo.2010.04.005, 2010.

Deng, J., Wang,C.M., and Li,G.J.: Style and processofthesuperimposedmineralization inthe Sanjiang Tethys, Acta Petrologica Sinica, 28 (5), 1349–1361 (in Chinese with Englishabstract), 2012.

Deng, J., Wang, Q.F., Li, G.J., and Santosh, M.: Cenozoic tectono-magmatic andmetallogenic processes in the Sanjiang region, southwestern China, Earth Sci.

Nonlin. Processes Geophys. Discuss., https://doi.org/10.5194/npg-2019-8
Manuscript under review for journal Nonlin. Processes Geophys.
Discussion started: 27 March 2019

Rev., 138, 268–299,https://doi.org/10.1016/j.earscirev.2014.05.015, 2014a.

Deng, J., Wang, Q.F., Li, G.J., Li, C.S., and Wang, C.M.: Tethys tectonic evolution and itsbearing on the distribution of important mineral deposits in the Sanjiang region,SW China, Gondwana Research, 26 (2), 419–437,https://doi.org/10.1016/j.gr.2013.08.002, 2014b.

Deng, J., Wang, Q.F., Li, G.J., Hou, Z.Q., Jiang, C.Z., and Danyushevsky, L.: Geology andgenesis of the giant Beiya porphyry–skarn gold deposit, northwestern YangtzeBlock, China, Ore Geol. Rev., 70, 457–485,https://doi.org/10.1016/j.oregeorev. 2015.02.015, 2015.

Emery, X.: Incorporating the uncertainty in geological boundaries into mineral resources evaluation, J. Geol. Soc. India, 69 (1), 29–38,2007.

Faure, K., Matsuhisa, Y., Metsugi, H., Mizota, C., and Hayashi, S.: The Hishikari Au–Agepithermal deposit, Japan: oxygen and hydrogen isotope evidence in determiningthe source of paleohydrothermal fluids, Economic Geology, 97, 481–498, https://doi.org/10.2113/gsecongeo.97.3.481, 2002.

Goovaerts, P.: Geostatistics for Natural Resources Evaluation, Oxford UniversityPress, New York, 496 pp. , 1997.

Goncalves, M. A., Mateus, A., and Oliveira, V.: Geochemicalanomaly separation by multifractal modeling, J. Geochem. Explor., 72, 91–114,https://doi.org/10.1016/S0375-6742(01)00156-X, 2001.

Hedenquist, J.W., Arribas, R.A., and Gonzalez-Urien, E.: Exploration for epithermal golddeposits, in: Hagemann, S.G. (Ed.), Gold in 2000: Reviews Economic Geology, 13, 245–277, 2000.

Hudson, D.M.: Epithermal alteration and mineralization in the Comstock District,Nevada, Economic Geology, 98, 367–385,2003.

Hoefs, J.: Stable Isotope Geochemistry, Springer-Verlag Berlin Heidelberg, Berlin, 2009.

Jensen, E.P. and Barton, M.D.: Gold deposits related to alkaline magmatism, Reviews Economic Geology, 13, 210–314, 2000.

Lowell, J.D.: Geology of the Kalamazoo orebody, San Manuel district, Arizona, Economic Geology, 63, 645–654, https://doi.org/10.2113/gsecongeo.63.6.645, 1968.

Lowell, J.D. and Guilbert, J.M.: Lateral and vertical alteration-mineralization zoning inporphyry ore deposits, Economic Geology, 65, 373–408, https://doi.org/10.2113/gsecongeo.65.4.373, 1970.

Li, C., Ma, T., and Shi, J.: Application of a fractal method relating concentrations anddistances for separation of geochemical anomalies from background, J. Geochem. Explor.,77, 167–175,https://doi.org/10.1016/S0375-6742(02)00276-5, 2003.

Li, W.C., Zeng, P.S., Hou, Z.Q., and White, N.C.: The Pulang porphyry copper deposit andassociated felsic intrusions in Yunnan Province, Southwest China, Economic Geology, 106 (1),79–92,https://doi.org/10.2113/econgeo.106.1.79 , 2011.

Leng, C.B., Zhang, X.C., Hu, R.Z., Wang, S.X., Zhong, H., Wang, W.Q., and Bi, X.W.: ZirconU–Pb and molybdenite Re–Os geochronology and Sr–Nd–Pb–Hf isotopic constraintson the genesis of the Xuejiping porphyry copper deposit in Zhongdian, NorthwestYunnan, China, Journal of Asian Earth Sciences ,60, 31–48, 2012.

Lin, X., Zhang,B., and Wang, X.: Application of factoranalysisand concentration–volumefractal modeling to delineation of 3D geochemical patterns: a case study of the Jinwozi gold field, NW China, Geochem. Explor. Environ. Anal., 14, 359–367, https://doi.org/10.1144/geochem2013-229, 2013.

Liu, X.L., Li, W.C., Yin, G.H., and Zhang, N.: The geochronology, mineralogy and geochemistry study of the Pulang porphyry copper deposits in Geza arc of Yunnan Province, Acta Petrologica Sinica, 29(9), 3049–3064 (in Chinese with English abstract), 2013.

Mandelbrot, B. B.: The Fractal Geometry of Nature, W. H. Freeman, San Fransisco, 468 pp., 1983.

Mao, S. and Journel, A.G.: Conditional 3D simulation of lithofacies with 2D seismic data, Comput. Geosci., 25(7), 845–862,https://doi.org/10.1016/S0098-3004(99)00006-0, 1999.

Melfos,V., Vavelidis,M., Christodes,G., and Seidel,E.: Origin and evolution of the Tertiary Maronia porphyry copper–molybdenum deposit, Thrace, Greece, Mineralium Deposita, 37, 648–668,https://doi.org/10.1007/s00126-002-0277-4, 2002.

Nonlin. Processes Geophys. Discuss., https://doi.org/10.5194/npg-2019-8
Manuscript under review for journal Nonlin. Processes Geophys.
Discussion started: 27 March 2019

Mao, J.W., Zhou, Z.H., Feng, C.Y., Wang, Y.T., Zhang, C.Q., Peng, H.J., and Yu, M.: A preliminary study of the Triassic large-scale mineralization in China and its geodynamicsetting, Geology in China, 39(6), 1437–1471 (in Chinese with English abstract), 2012.

Mao, J.W., Pirajno, F., Lehmann, B., Luo, M.C., and Berzina, A.: Distribution of porphyrydeposits in the Eurasian continent and their corresponding tectonic settings, Journal of Asian Earth Sciences, 79(PartB), 576–584, https://doi.org/10.1016/ j.jseaes.2013.09.002, 2014.

Pirajno, F. and Bagas, L.: Gold and silver metallogeny of the South China Fold Belt: a consequence of multiple mineralizing events? Ore Geol. Rev., 20, 109–126,https://doi.org/10.1016/S0169-1368(02)00067-7, 2002.

Pirajno, F.: Hydrothermal Processes and Mineral Systems, Springer, The Universityof Western Australia, Perth, 2009.

Pang, Z.S., Du, Y.S., Wang, G.W., Guo, X., Cao, Y., and Li, Q.: Single-grain zircon U–Pb isotopic ages, geochemistry and its implication of Pulang complex in Yunnan Province,China, Acta Petrologica Sinica, 25(1), 159–165(in Chinese with English abstract), 2009.

Pyrcz, M.J. and Deutsch, C.V.: Geostatistical ReservoirModeling, OxfordUniversity Press, 2014.

Richards, J.P.: Alkalic-type epithermal gold deposits, Min. Assoc. Canada, ShortCourse, 23, 367–400, 1995.

Reis, A., Sousa, A., and Cardoso Fonseca, E.: Application of geostatistical methods in gold geochemical anomalies identification (Montemor-O-Novo,Portugal), J. Geochem.Explor., 77(1), 45–63, https://doi.org/10.1016/S0375-6742(02)00269-8, 2003.

Schwartz, G.M.: Hydrothermal alteration in the “porphyry copper” deposits, Economic Geology, 42, 319–352, https://doi.org/10.2113/gsecongeo.42.4.319, 1947.

Sillitoe, R.H. and Gappe, I.M.: Philippine porphyry copper deposits: geologic settingand characteristics, Common Coordination Joint Resource (CCOP),14, 1–89, 1984.

Nonlin. Processes Geophys. Discuss., https://doi.org/10.5194/npg-2019-8
Manuscript under review for journal Nonlin. Processes Geophys.
Discussion started: 27 March 2019

Nonlinear Processes in Geophysics
Discussions

Sillitoe, R.H.: Characteristics and controls of the largest porphyry copper–gold andepithermal gold deposits in the circum-pacific region, Australian Journal of Earth Sciences, 44, 373–388, https://doi.org/10.1080/08120099708728318, 1997.

Sim,B.L.,Agterberg,F.P.,andBeaudry,C.:Determiningthecutoffbetween background and relative base metal contamination levels using multifractal methods, Comput. Geosci., 25, 1023–1041,1999.

Stegman, C.L.: How Doman Envelopes Impact on ihc Resource Estimate—Case Studiesfrom the Cobar Gold Field, NSW, Australia, in: Mineral Resource and Ore ReserveEstimation—the AusIMM Guide to Good Practice, Edwards, A.C. (Ed.), TheAustralasian Institute of Mining and Metallurgy: Melbourne,221–236, 2001.

San Shen, J.J. and Yang, H.J.: Sources and genesis of the Chinkuashih Au–Cu depositsin northern Taiwan: constraints from Os and Sr isotopic compositions of sulfides, Earth and Planetary Science Letters, 222, 71–83,https://doi.org/10.1016/j.epsl.2004.02.029, 2004.

Subbey, S., Christie, M., and Sambridge, M.: Prediction under uncertainty in reservoirmodeling, J. Pet. Sci. Eng., 44(1), 143–153, https://doi.org/10.1016/j.petrol.2004.02.011, 2004.

Spalla, M.I., Morotta, A.M., and Gosso, G.: Advances in interpretation of geologicalprocesses: refinement of multi-scale data and integration in numerical modelling, Geological Society, London, 240 pp., 2010.

Sadeghi, B., Moarefvand, P., Afzal, P., Yasrebi, A.B., and Saein, L.D.: Application of fractalmodels to outline mineralized zones in the Zaghia iron ore deposit, Central Iran, J. Geochem. Explor., 122, 9–19,https://doi.org/10.1016/j.gexplo.2012.04.011, 2012.

Soltani, F., Afzal, P., and Asghari, O.: Delineation of alteration zones based on SequentialGaussian Simulation and concentration–volume fractal modeling in the hypogenezone of Sungun copper deposit, NW Iran, J. Geochem. Explor., 140, 64–76, https://doi.org/10.1016/j.gexplo.2014.02.007, 2014.

Sun, T. and Liu, L.: Delineating the complexity of Cu-Mo mineralization in a porphyryintrusion by computational and fractal modeling: A case study of the Chehugoudeposit in the Chifeng district, Inner Mongolia, China, J. Geochem. Explor.,

Nonlinear Processes in Geophysics
Open Access
Discussions

144,128–143,https://doi.org/10.1016/j.gexplo.2014.02.015, 2014.

Turcotte, D.L.: A fractal approach to the relationship between ore grade andtonnage, Economic Geology, 18, 1525–1532, 1986.

Turcotte, D. L.: Fractals in geology and geophysics, Pure Appl.Geophys., 131, 171–196, 1989.

White, N.C. and Hedenquist, J.W.: Epithermal gold deposits: styles, characteristicsand exploration, SEG Newsletter, 23, 1–14, 1995.

Wilson, A.J., Cooke, David, R., Harper, B.J., and Deyell, C.L.: Sulfur isotopic zonation inthe Cadia district, southeastern Australia: exploration significance and implications for the genesis of alkalic porphyry gold–copper deposits, Mineralium Deposita, 42, 465–487,https://doi.org/10.1007/s00126-006-0071-9, 2007.

Wang, Q.F., Deng, J., Liu, H., Wang, Y., Sun, X., and Wan, L.: Fractal models for estimatinglocal reserves with different mineralization qualities and spatial variations, J. Geochem. Explor., 108, 196–208, https://doi.org/10.1016/j.gexplo.2011.02.008, 2011.

Wang, Q.F., Deng, J., Li, C.S., Li, G.J., Yu, L., and Qiao, L.: The boundary between the Simaoand Yangtze blocks and their locations in Gondwana and Rodinia: constraints from detrital and inherited zircons, Gondwana Research, 26(2), 438–448,https://doi.org/10.1016/j.gr.2013.10.002, 2014.

Wang, G. W., Emmanuel John M. Carranza,Zuo, R., Hao, Y. L., Du, Y. S., Pang, Z. S., and Sun Y.: Mapping of district-scale potential targets using fractal models, J. Geochem. Explor., 122, 34–46,https://doi.org/10.1016/j.gexplo.2012.06.013, 2012.

Yamamoto, J.K.: Comparing Ordinary Kriging Interpolation Variance and Indicator Kriging Conditional Variance for Assessing Uncertainties at Unsampled Locations, in: Application ofComputers and Operations Research in the Mineral Industry,edited by: Dessureault, S., Ganguli, R., Kecojevic, V., and Girard-Dwyer, J., Balkema, 2005.

Yunnan Diqing Nonferrous Metal Co. Ltd.: Exploration Report of Pulang Copper Deposit, Diqing, Yunnan, China, Yunnan Diqing Nonferrous Metal Co. Ltd., DiqingTibetan Autonomous Prefecture (in Chinese), 2009.

Zeng, P.S., Hou, Z.Q., Li, L.H., Qu, W.J., Wang, H.P., Li, W.C., Meng, Y.F., and Yang, Z.S.: Age of the Pulang porphyry copper deposit in NW Yunnan and its geological significance, Geological Bulletin of China, 23(11), 1127–1131 (in Chinese with English abstract), 2004.

Zuo, R., Cheng, Q., and Xia, Q.: Application of fractal models to characterization of vertical distribution of geochemical element concentration, J. Geochem. Explor., 102, 37–43,https://doi.org/10.1016/j.gexplo.2008.11.020, 2009.

Zuo, R., Carranza, E.J.M., and Cheng, Q.: Fractal/multifractal modelling of geochemical exploration data, J. Geochem. Explor., 122, 1–3, https://doi.org/10.1016/j.gexplo.2012.09.009, 2012.

Zuo, R. and Wang, J.: Fractal/multifractal modeling of geochemical data: A review, J. Geochem. Explor., 164, 33-41, https://doi.org/10.1016/j.gexplo.2015.04.010, 2016.

Fig.1. Geological map of the Pulang porphyry copper deposit, SW China.Modified after Yunnan Diqing Nonferrous Metal Co. Ltd., 2009.

Fig.2. Geological 3D models including lithology, alterationand 3Ddrillholeplot with the legend of each in thePulang porphyry copper deposit. (Scale is in m^3.)

Fig.3. Photographs of alteration and mineralization in the Pulang porphyry copper deposit, SW China. (a) Quartz monzonite porphyry with potassium-silicate alteration; (b) Quartz diorite porphyrite with quartz-sericite alteration; (c) Quartz diorite porphyrite with propylitic alteration; (d) Hornfels. Qtz=quartz; Pl=plagioclase; Kfs=K-feldspar; Bt=biotite; Ser=sericite; Chl=chlorite; Ep=epidote; Py=pyrite; Ccp=chalcopyrite; Mo=molybdenite; Po= pyrrhotite.

Fig.4. Cross section along exploration line 0 in the Pulang porphyry copper deposit, SW China. Modified after Wang et al., 2012.

Fig.5. Histogram of Cu concentrations in lithogeochemical samples from the Pulang deposit.

Fig.6. The experimental semi–variogram (omni-directional) of Cu data in Pulang deposit.

Fig.7. C–V log–log plot for Cu concentrations in the Pulang deposit.

Fig.8. Zones in the Pulang deposit based on thresholds defined from the C–V fractal model of Cu data: (a) highly mineralized zones; (b) moderately mineralized zones; (c) weakly mineralized zones; (d) barren host rock.(Scale is in m^3.)

Fig.9. S–V log–log plot for Cu concentrations in the Pulang deposit.

Fig.10. Zones in the Pulang deposit based on thresholds defined from the S–V fractal model of Cu data: (a) the supergene enrichment zones; (b) the hypogene zones; (c) the leached zone and barren host rock (Scale is in m^3.)

Fig.11. Highly mineralized zones in the Pulang deposit: (a) potassium-silicate zone resulted from the 3D geological model from drillcore geological data; (b) C–V modeling of Cu data; and (c) S–V modeling of Cu data(Scale is in m^3.)

Fig.12. Moderately mineralized zones in the Pulang deposit:(a) quartz–sericite zones resulted from the 3D geological model from drillcore geological data; (b) C–V modeling of Cu data; and (c)S–V modeling of Cu data (Scale is in m^3.)

Fig.13. Chalcopyrite content in several samples based on mineralographical study: (a) PL-B82 sample collected from supergene enrichment zones; (b) PL-B62 sample collected from the hypogene zones; (c) PL-B74 sample collected from the hypogene zones; (d) PL-B94 sample collected from leached zone and barren host rock.
Po= pyrrhotite; Ccp=chalcopyrite.

Table 1 Thresholds concentrations obtained by using C–V model based on Cu% in Pulang deposit.

Table 2 Ranges of power spectrum (S) for different mineralization zones in Pulang deposit.

Table 3 Matrix for comparing performance of fractal modeling results with geological model. A, B, C, and D represent numbers of voxels in overlaps between classes in the binary geological model and the binary results of fractal models (Carranza, 2011).

Table 4 Overall accuracy (OA), Type I and Type II errors (T1E and T2E, respectively) with respect to potassic alteration zone resulted from geological model and threshold values of Cu obtained through C–V and S–V fractal modeling.

Table 5 Overall accuracy (OA), Type I and Type II errors (T1E and T2E, respectively) with respect to phyllic alteration zone resulted from geological model and threshold values of Cu obtained through C–V and S–V fractal modeling.

Nonlin. Processes Geophys. Discuss., https://doi.org/10.5194/npg-2019-8
Manuscript under review for journal Nonlin. Processes Geophys.
Discussion started: 27 March 2019

Nonlinear Processes in Geophysics
Open Access
Discussions

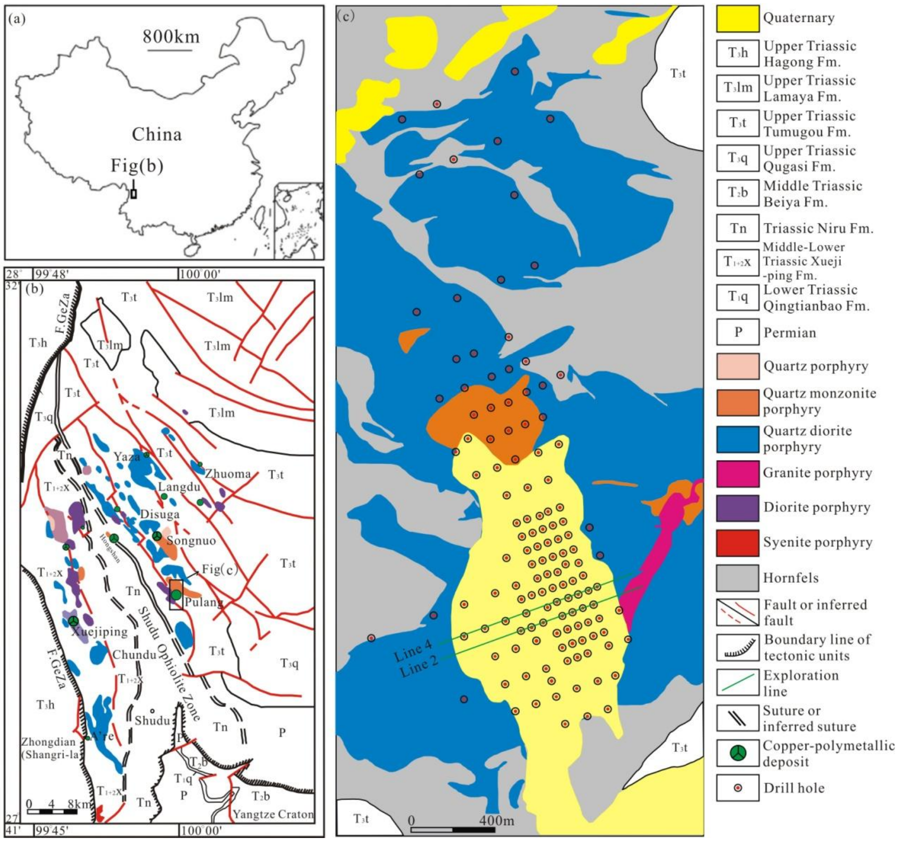

Fig. 1.

Nonlin. Processes Geophys. Discuss., https://doi.org/10.5194/npg-2019-8
Manuscript under review for journal Nonlin. Processes Geophys.
Discussion started: 27 March 2019

Nonlinear Processes in Geophysics
Discussions

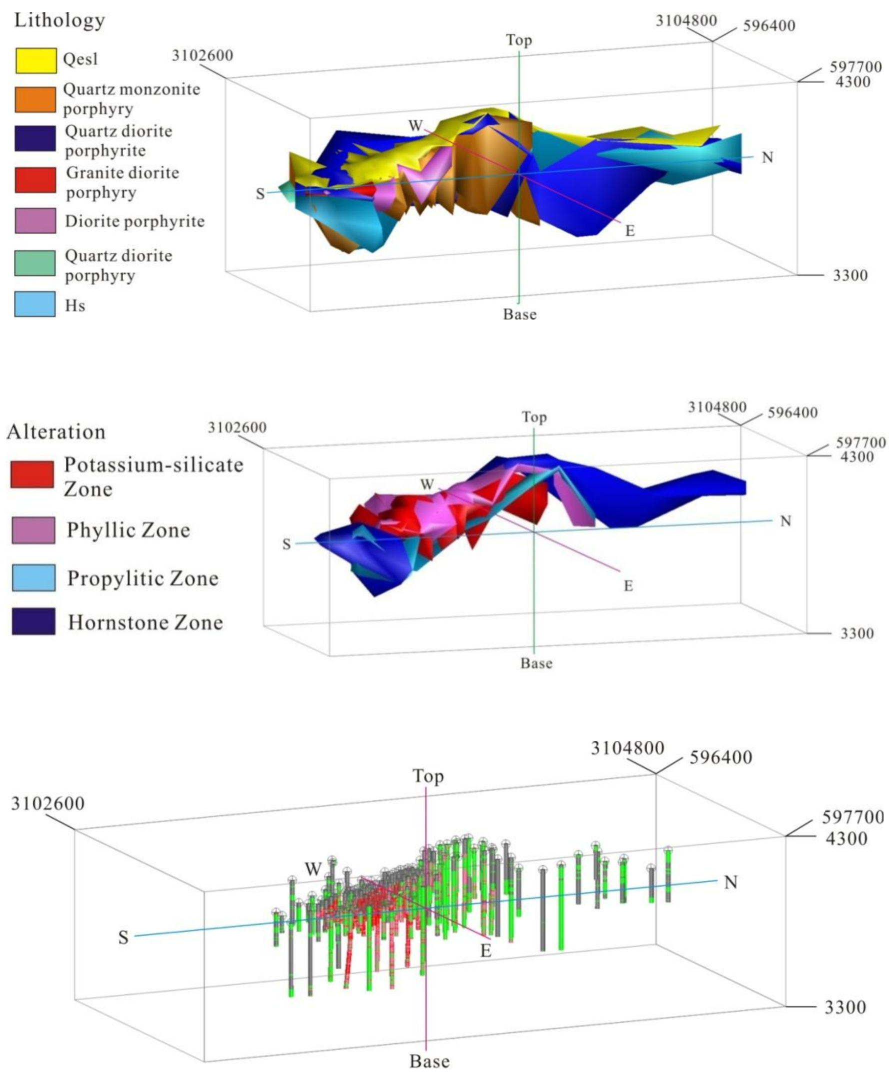

Fig. 2.

Nonlinear Processes in Geophysics
Discussions

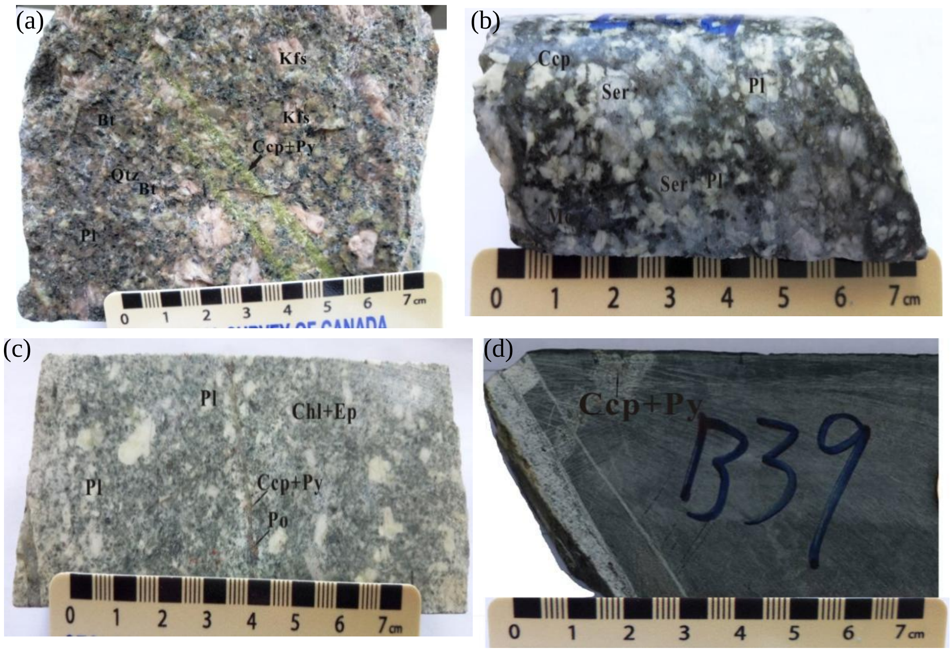

Fig. 3.

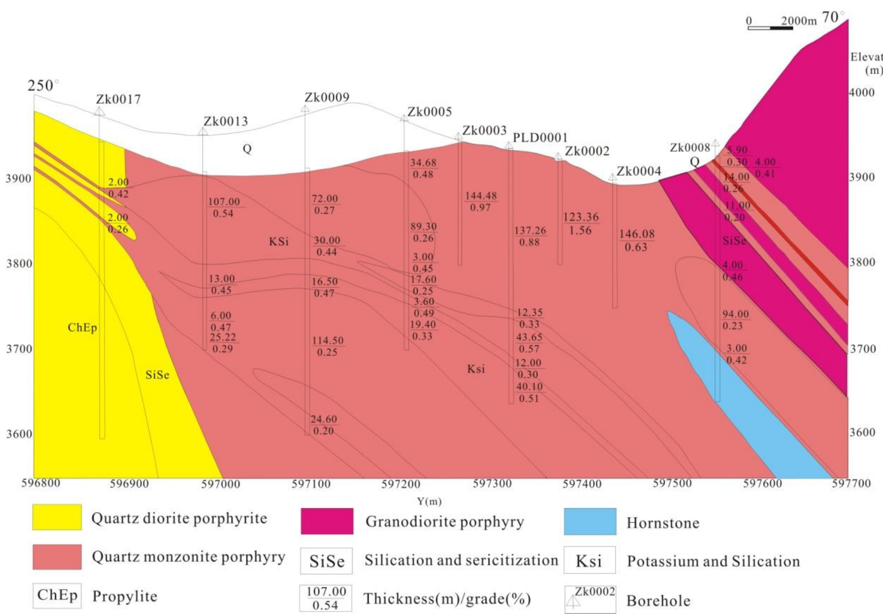

Fig. 4.

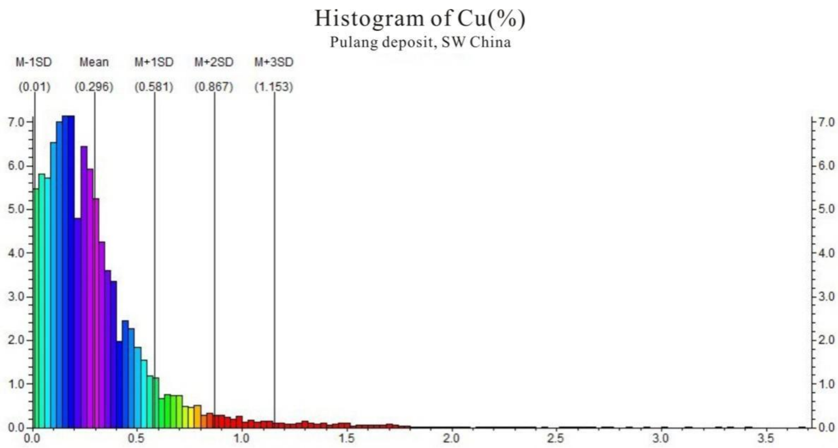
Histogram of Cu(%)
Pulang deposit, SW China
M-1SD (0.01)
Mean (0.296)
M+1SD (0.581)
M+2SD (0.867)
M+3SD (1.153)

Fig. 5.

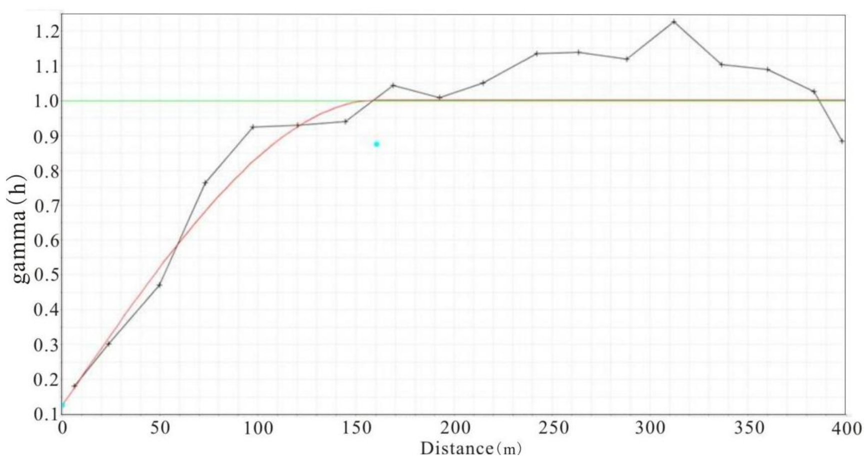
gamma (h)
Distance (m)

Fig. 6.

Nonlinear Processes in Geophysics
Discussions
Open Access

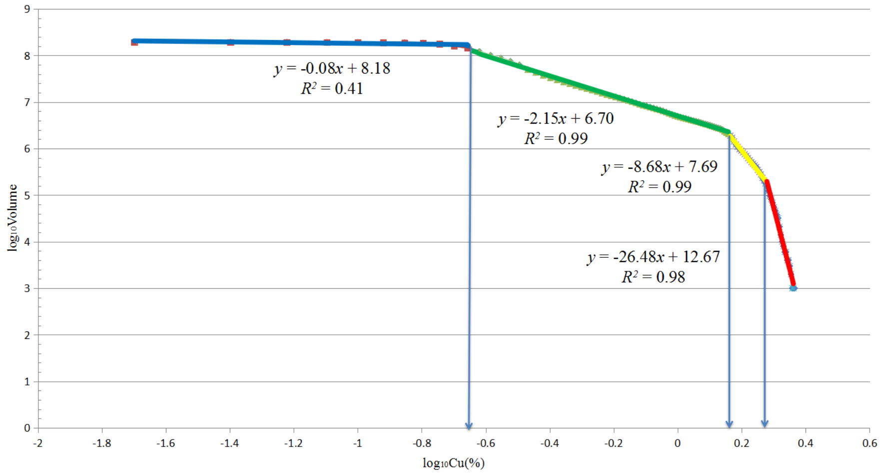

Fig. 7.

(a)

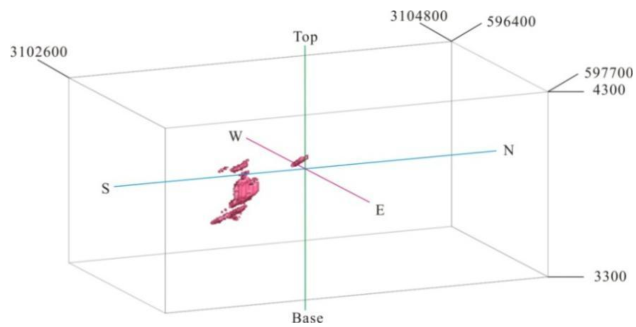
3102600
Top
3104800
596400
597700
4300
W
N
S
E
3300
Base

(b)

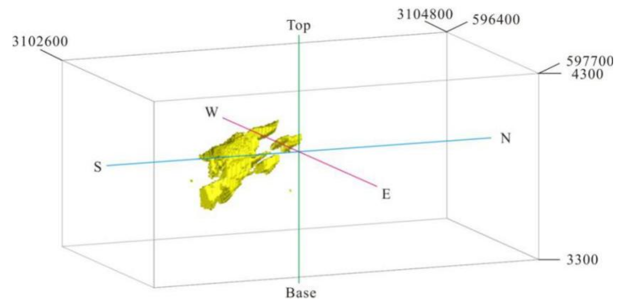
3102600
Top
3104800
596400
597700
4300
W
N
S
E
3300
Base

(c)

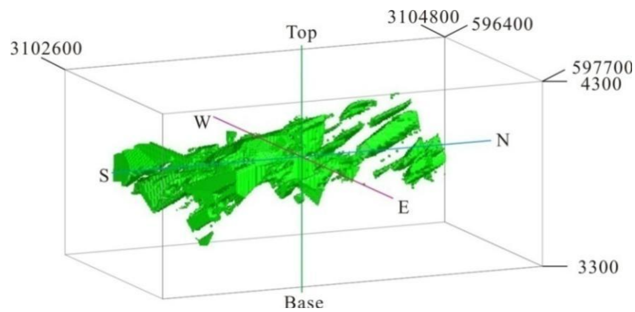
3102600
Top
3104800
596400
597700
4300
W
N
S
E
3300
Base

(d)

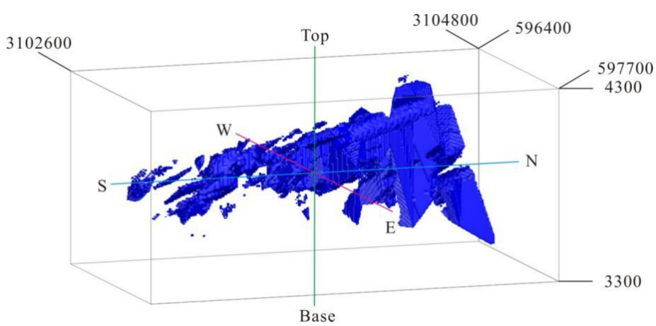
3102600
Top
3104800
596400
597700
4300
W
N
S
E
3300
Base

Fig. 8.

Nonlin. Processes Geophys. Discuss., https://doi.org/10.5194/npg-2019-8
Manuscript under review for journal Nonlin. Processes Geophys.
Discussion started: 27 March 2019

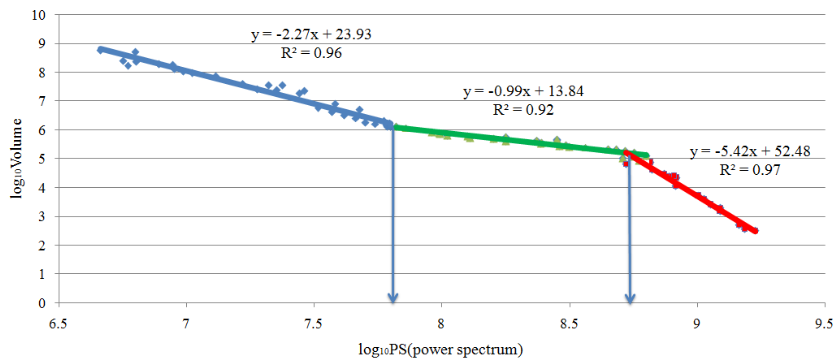

Fig. 9.

(a)

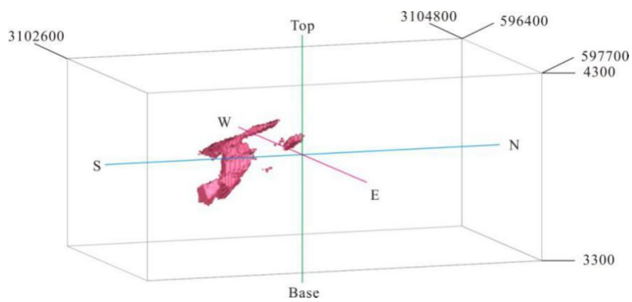

(b)

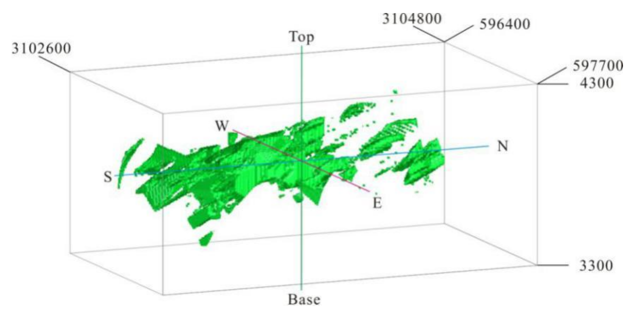

(c)

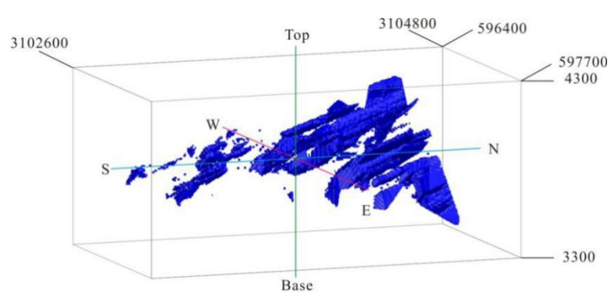

Fig. 10.

Nonlin. Processes Geophys. Discuss., https://doi.org/10.5194/npg-2019-8
Manuscript under review for journal Nonlin. Processes Geophys.
Discussion started: 27 March 2019

Nonlinear Processes in Geophysics
Discussions

(a)

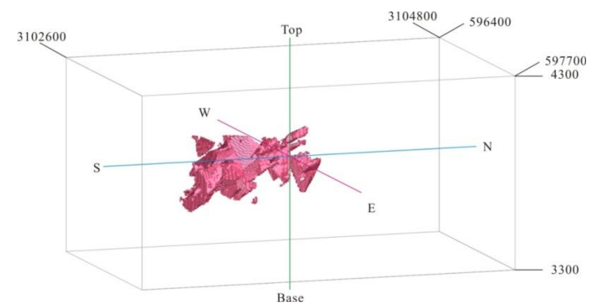

(b)

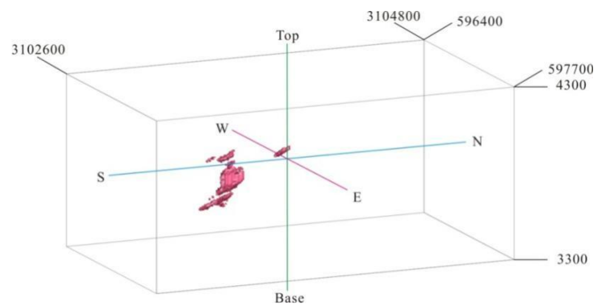

(c)

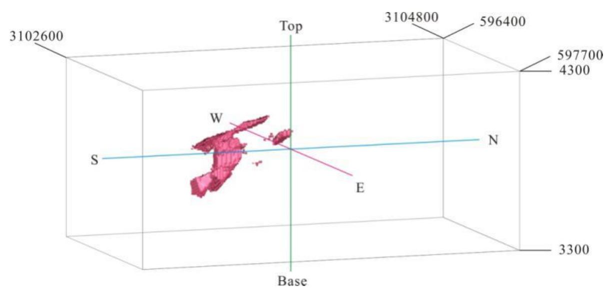

Fig. 11.

Nonlin. Processes Geophys. Discuss., https://doi.org/10.5194/npg-2019-8
Manuscript under review for journal Nonlin. Processes Geophys.
Discussion started: 27 March 2019

Nonlinear Processes in Geophysics
Open Access
Discussions

(a)

(b)

(c)

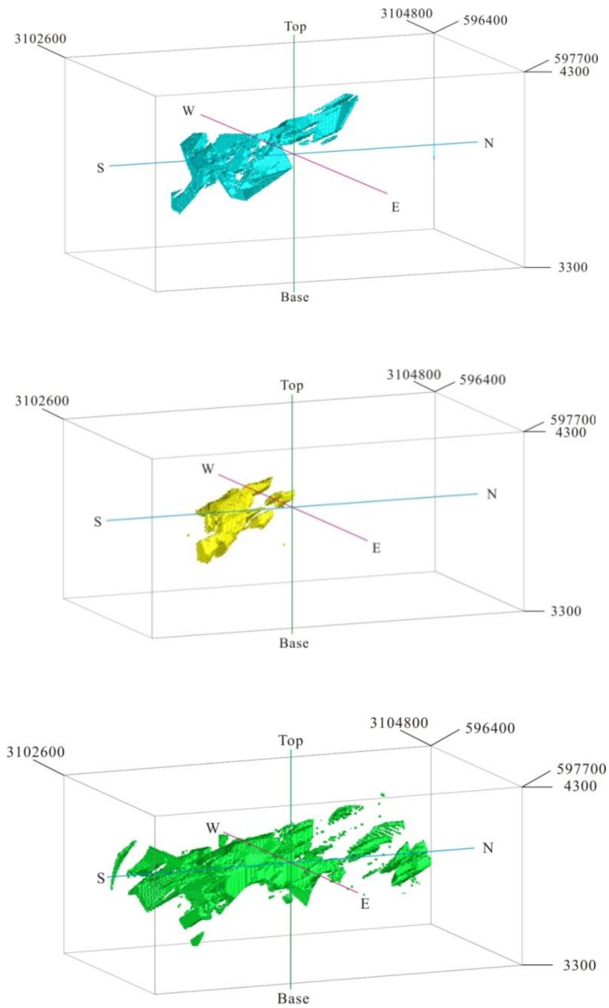

Fig. 12.

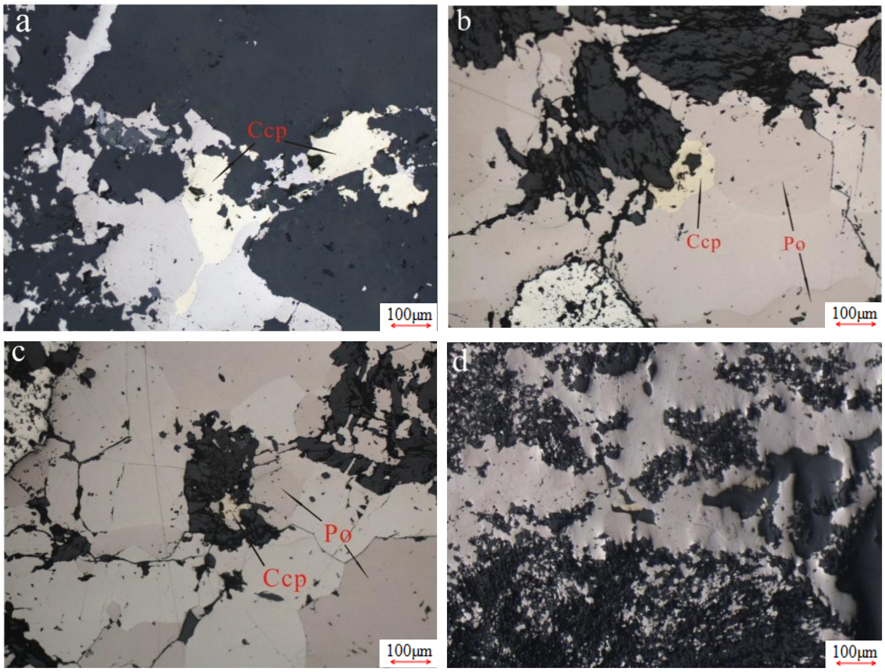

Fig. 13.

Nonlin. Processes Geophys. Discuss., https://doi.org/10.5194/npg-2019-8
Manuscript under review for journal Nonlin. Processes Geophys.
Discussion started: 27 March 2019

Nonlinear Processes in Geophysics
Discussions
Open Access
EGU

Table 1

Mineralized zones	Thresholds(Cu%)	Range(Cu%)
Barren host rock		<0.25
Weakly mineralized	0.25	0.25–1.38
Moderately mineralized	1.38	1.38–1.88
Highly mineralized	1.88	>1.88

Table 2

Mineralized zones	PS threshold	Range of PS	Range(Cu%)
leached zone and barren host rock		<7.81	<0.23
hypogene zones	7.81	7.81-8.70	0.23-1.33
supergene enrichment zones	8.70	>8.70	>1.33

Table 3

		Geological model	
		Inside zone	Outside zone
Fractal model	Inside zone	True positive (A)	False positive (B)
	Outside zone	False negative (C)	True negative (D)
		TypeIerror=C/(A+C)	TypeIIerror=B/(B+D)
		Overallaccuracy=(A+D)/(A+B+C+D)	

Table 4

		Potassic alteration of geological model	
		Inside zones	Outside zones
C–V fractal model of highly mineralized zones	Inside zones	A 2850	B 1360
	Outside zones	C 77927	D 76913
		T1E 0.96	T2E 0.02
		OA	0.50
S–V fractal model of supergene enrichment zones	Inside zones	A 4131	B 2318
	Outside zones	C 73985	D 74726
		T1E 0.95	T2E 0.03
		OA	0.52

Nonlinear Processes in Geophysics
Discussions
Open Access
EGU

Table 5

		Phyllic alteration of geological model	
		Inside zones	Outside zones
C–V fractal model of moderately and weakly mineralized zones	Inside zones Outside zones	A 36518 C 25461 T1E 0.41 OA	B 48027 D 69155 T2E 0.40 0.59
S–V fractal model of the hypogene zones	Inside zones Outside zones	A 40080 C 26899 T1E 0.40 OA	B 44943 D 54239 T2E 0.45 0.56